

Alma Mater Studiorum Università di Bologna
Archivio istituzionale della ricerca

Mobile cobots for autonomous raw-material feeding of automatic packaging machines

This is the final peer-reviewed author's accepted manuscript (postprint) of the following publication:

Published Version:

Comari S., Di Leva R., Carricato M., Badini S., Carapia A., Collepalambo G., et al. (2022). Mobile cobots for autonomous raw-material feeding of automatic packaging machines. JOURNAL OF MANUFACTURING SYSTEMS, 64, 211-224 [10.1016/j.jmsy.2022.06.007].

Availability:

This version is available at: <https://hdl.handle.net/11585/890632> since: 2022-07-13

Published:

DOI: <http://doi.org/10.1016/j.jmsy.2022.06.007>

Terms of use:

Some rights reserved. The terms and conditions for the reuse of this version of the manuscript are specified in the publishing policy. For all terms of use and more information see the publisher's website.

This item was downloaded from IRIS Università di Bologna (<https://cris.unibo.it/>).
When citing, please refer to the published version.

(Article begins on next page)

This is the final peer-reviewed accepted manuscript of:

*Simone Comari, Roberto Di Leva, Marco Carricato, Simone Badini, Alessandro Carapia, Giacomo Collepalambo, Andrea Gentili, Claudio Mazzotti, Katia Staglianò, Dario Rea, **Mobile cobots for autonomous raw-material feeding of automatic packaging machines**, Journal of Manufacturing Systems, Volume 64, 2022, Pages 211-224, ISSN 0278-6125*

The final published version is available online at:

<https://doi.org/10.1016/j.jmsy.2022.06.007>

Rights / License:

The terms and conditions for the reuse of this version of the manuscript are specified in the publishing policy. For all terms of use and more information see the publisher's website.

This item was downloaded from IRIS Università di Bologna (<https://cris.unibo.it/>)

When citing, please refer to the published version.

Mobile Cobots for Autonomous Raw-material Feeding of Automatic Packaging Machines

Simone Comari^{a,*}, Roberto Di Leva^a, Marco Carricato^{a,**}, Simone Badini^b,
Alessandro Carapia^b, Giacomo Collepalumbo^b, Andrea Gentili^b, Claudio Mazzotti^b,
Katia Staglianò^b and Dario Rea^b

^aDIN - Department of Industrial Engineering, Viale del Risorgimento 2, Bologna, 40136, Italy

^bIMA - Industria Macchine Automatiche s.p.a., Via Emilia, 428/442, Ozzano dell'Emilia (Bologna), 40064, Italy

ARTICLE INFO

Keywords:

Machine Tending
Robotic manipulation
Mobile robots
Collaborative robots
Computer vision
Trajectory planning
Mechanical design
Industry 4.0

ABSTRACT

Human-robot collaboration has become a key driver for manufacturing sustainability in Europe. Thanks to the many advantages that a fenceless, shared working environment offers, industry has recently grown a particular interest in collaborative robotics, thus sustaining the transition from academy to factories of this technology. In this work, we present a robotic solution integrating a serial manipulator and a mobile platform, both characterized by collaborative features, for feeding raw material to a packaging automatic machine. The goal is to provide an overview of such a complex system from different points of view, including hardware and software architecture, trajectory planning, computer-vision strategies, customized mechanical design, and field validation. We will describe the obtained results and the lessons learned, and provide an outlook for future evolution.

1. Industrial Context

Human-Robot collaboration has become a key driver for manufacturing sustainability in Europe. Low installation and running costs, and a high degree of flexibility are the main characteristics that make collaborative robots (cobots¹) appealing to many companies seeking out re-shoring production facilities with a short Return On Investment (Bortolini, Ferrari, Gamberi, Pilati and Faccio, 2017), (euf, 2018). Moreover, the ageing of the workforce poses a dramatic challenge to health and safety in all European countries (Magnavita, 2017). In this context, cobots can become a support and an extension of human capabilities, thus relieving operators from repetitive, alienating and/or heavy operations, leaving them in charge of more complex tasks, where experience can assume predominant importance and greater efficacy. Cobots can be installed in a fenceless but completely safe shared environment, thus leaving the factory's layout and facilities almost unaffected.

While industrial robotics has been heavily employed in the past decades, collaborative robotics, despite being an available technology since the early 2000s, prominently entered the industrial scene just recently (Pedrocchi, Vicentini, Matteo and Tosatti, 2013). Given their versatility and inherent characteristic of not needing any protective barrier surrounding them, it was not long before researchers realized it was a good idea to install them on mobile platforms to freely move them around to perform different jobs. Moreover, a single mobile robot can replace many stationary robots that would otherwise only be operational for a short period of time, thus considerably reducing the fixed costs of a production line. Among the first examples of integrated mobile robots and robotic manipulators for industry-oriented tasks, Berntorp, Arzen and Robertsson (2012) and Nieuwenhuisen, Droeschel, Holz, Stuckler, Berner, Li, Klein and Behnke (2013) designed and developed original robotic systems able to navigate and operate in a specific environment (e.g. a grocery store (Berntorp et al., 2012)) and perform a complex task (e.g. bin picking (Nieuwenhuisen et al., 2013)). The Robo-Partner EU project (Michalos, Makris, Spiliotopoulos, Misios, Tsarouchi and Chryssolouris, 2014) focused on combining the capacities and cognitive abilities of humans with the robot strength, velocity, repeatability

*e-mail: simone.comari@unibo.it, postal address: Via Terracini 24, 40131, Bologna, Italy

**e-mail: marco.carricato@unibo.it, postal address: Viale del Risorgimento 2, 40136, Bologna, Italy

ORCID(s): 0000-0003-0562-8799 (S. Comari); 0000-0002-7469-0345 (R. Di Leva); 0000-0002-1528-4304 (M. Carricato); 0000-0001-8870-8406 (S. Badini); 0000-0001-9952-4143 (A. Carapia); 0000-0001-9576-0675 (G. Collepalumbo); 0000-0002-6779-8825 (C. Mazzotti); 0000-0002-8526-5328 (K. Staglianò); 0000-0002-5684-729X (D. Rea)

¹The term "cobot" was coined in 1996 by J. E. Colgate and M. Peshkin, professors at Northwestern University, who issued a homonym US patent in 1997 to describe this new technology.

and precision in the assembly of the rear axle of a passenger vehicle, developing intuitive human-robot interfaces using sensors, visual servoings, speech recognition, and advanced control algorithms. Krug, Stoyanov, Tincani, Andreasson, Mosberger, Fantoni and Lilienthal (2016) addressed the automatization of order picking procedures, investigating the use case of autonomous picking and palletizing by means of a dedicated mobile platform equipped with an industrial cobot. The Valeri EU project (SAENZ, PENZLIN, VOGEL and FRITZSCHE, 2016) aimed at testing mobile robotics in the aerospace industry. The Kuka's omniRob platform was used and supplemented with a rotating vertical linear axis on which a lightweight manipulator was mounted. Tactile sensors and a 2½D vision system were employed to establish a safe space around the tool, in order to robustly detect humans or unknown objects intruding into this safety area. In Dömel, Kriegel, Kassecker, Brucker, Bodenmüller and Suppa (2017), a similar robotic system to the one employed in this work was used and equipped with multiple perceptive sensors to perform manipulation tasks in a water pump production site. In Unhelkar, Dörr, Bubeck, Lasota, Perez, Siu, Boerkoel, Tyroller, Bix, Bartscher and Shah (2018), the authors presented a mobile robotic system designed for operating on the moving floors of automotive final assembly lines. A different navigation and planning paradigm is described in Iriondo, Lazkano, Susperregi, Urain, Fernandez and Molina (2019), where deep reinforcement learning was selected to perform collision-free trajectories for pick-and-place operations in highly unstructured areas, such as a logistic facility. Lastly, a comprehensive review of system architectures and applications in the field of collaborative mobile industrial manipulators is given in Yang, Yang, Zante, Post and Liu (2019) whereas a most recent work by Bi et al. Bi, Luo, Miao, Zhang, Zhang and Wang (2021) discusses the main challenges and methods related to safety assurance when dealing with cobots by listing relevant examples and successful case studies.

The goal of the work presented here consists in employing a combination of a serial manipulator and a mobile platform, both characterized by collaborative features, in order to automatize the raw-material feeding operation to a tea-packaging automatic machine. We show how an ad-hoc architecture built with industrial components can represent a marketable solution to a specific machine tending task. With weights up to 12 kg, the repeated loading of raw materials can become a source of physical distress for a human operator in the long run. Moreover, the operator must always interrupt his/her main job to take care of this short task, leading to a continuous loss of concentration. On the other hand, the number of times that this operation must be executed over a working shift is not sufficient to justify the investment of many standard de-palletizer robots, each one installed next to an automatic machine. A more dynamic automatic solution may be preferred, namely, a single mobile robotic system that is able to self-navigate and serve many machines when needed, while, at the same time, relieving the operators from this occasional burden. Nowadays, robot and tool manufacturers offer a wide range of options for inherent collaborative robots which can serve many purposes. Such systems have been widely used in the laboratory framework but they barely find application in real-case scenarios, except for a few project-oriented innovation actions driven by special fundings and with limited scope. The presented work describes how the integration of these complex systems led to the achievement of a marketable, resilient and durable technology, hence breaking the barriers between academy and industry. In particular, conveniently-chosen procedures allow the system to easily recover from errors, and the planning of specific manipulation strategies, together with the design of customized mechanical components, permits the handling of raw materials, which differ in shape and weight. This way, the robotic system is capable of efficiently managing the arbitrariness of an unstructured environment while maintaining high safety standards for the human operators working nearby.

The project described in this paper builds up from a previous work developed for the European Robotics Challenges (EuRoC) by the TIMAIRIS team (Pedrosa, Lim, Amaral, Pereira, Cunha, Azevedo, Dias, Dias, Reis, Shafii, Tudico, Mazzotti, Carricato, Badini, Rea and Lau, 2020) between 2014 and 2018, where autonomous feeding of cardboard blanks for the same packaging machine was investigated, and the first trials of blanks' pick-up operation were performed by using the envisioned robotic system. With the MaXima (Multiple Actions for Innovation in Machine Automation) project, developed between 2016 and 2019, IMA s.p.a., in collaboration with the Department of Industrial Engineering (DIN) of the University of Bologna, brings the results and lessons learned in the challenge into a real-case scenario, with the aim of automatizing the change of not only blanks but also raw-material reels, and making the robotic system better suited for industrial use, and thus, marketable.

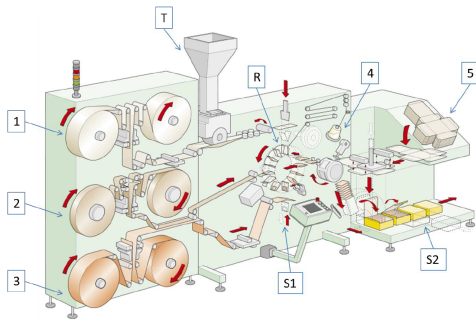
The proposed solution is described in Section 2, followed by a brief insight into safety standards and features in Section 3. Section 4 is dedicated to the high-level architecture of the working cell, including the main communication protocols. Sections 5 and 6 describe trajectory-planning strategies for the mobile platform and the manipulator, respectively, whereas Section 7 focuses on customized mechanical components. Section 8 gives an overview of the computer-vision solutions implemented for the project needs. Section 9 describes field experimentation and provides an outlook on future evolution and improvements. Finally, Section 10 draws conclusions.

Table 1

Description of functional scheme of C24-E (Figure 1a).

Ref. Num.	Name	Description	Notes
1	filter paper reels	-	Maximum weight = 7.1 Kg.
2	tag reels	-	Maximum weight = 5 Kg.
3	outer envelope reels	-	Maximum weight = 12 Kg.
4	thread spool	-	-
5	stack of <i>blanks</i>	Blanks are pre-shaped packaging cardboard that will form the boxes containing the tea bags.	-
T	hopper	It feeds the tea onto the filter paper.	-
R	formation wheel	Rotation element designated to the tea bag formation, adding both tag and thread.	-
S1-S2	ejection sections	Sections of the machine responsible for ejecting defective units.	-

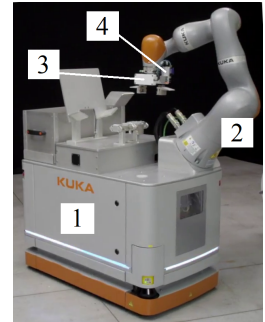
2. Robotic System Description



(a) Functional scheme of C24-E automatic machine



(b) The local storage wagon



(c) AMR

Figure 1: Robotized production cell elements.

Throughout this article, we use the term *Autonomous Mobile Robot* (AMR) to define the set of main components that characterize the robotic system at hand. Moreover, we define *robotized production cell* (Figure 1) the set of the following elements of the plant:

- (a) an *automatic packaging machine*;
- (b) a local storage for stocking raw material necessary for a single working shift;
- (c) an AMR responsible for feeding raw material and monitoring the process.

In Sections 2.1, 2.2 and 2.3, we describe the aforementioned components in detail.

2.1. Automatic Tea Packaging Machine

C24-E² is a fully automatic machine for packaging tea bags sealed with a double knot, coming with wire and a hard tag. C24-E may produce a wide variety of tea bags and boxes, and it can reach the maximum speed of 400 bags per minute. Figure 1a shows a simplified representation of C24-E and the raw material to be fed to the machine, whose main elements are described in Table 1.

²For more details, please visit <https://ima.it/beverage/machine/c24-e/>

2.2. Local Raw-Material Storage Wagon

A *local storage wagon* (or simply *wagon* in the following) (Figure 1b) located close to a rack of automatic machines is a common strategy adopted by several IMA clients. It acts as an intermediate storing station between the actual warehouse and the automatic machines, and can contain enough reels and blanks for a whole working shift. In order to decrease the impact of the new robotic system on the plant, we opted for maintaining this paradigm. However, we revisited the design of this wagon to simplify the interaction with the AMR. Top shelves are optimized for carrying a pile of filter-paper reels and a pile of outer-envelope reels, slightly tilted to ensure stability. A similar concept is used for the bottom shelves, suitably arranged to allocate a pile of tag reels and another pile of outer-envelope reels. On the side, there is a slot suited for a pallet of blanks, properly stacked to maximise the number of available items. The wagon can be manually moved thanks to lockable castor wheels and brought to the warehouse for refill. Due to this reason, the wagon position is never perfectly known, and therefore marker tags are used to help the vision system to accurately locate the wagon pose, after a first location refinement is carried out by the AGV by exploiting laser-scanner readings and the knowledge of the 3D shape of the wagon (see Sections 6.1 and 8.2).

2.3. Autonomous Mobile Robot

With reference to the numbering in Fig. 1c, the AMR consists of:

1. an *Automated Guided Vehicle* (AGV) that allows the AMR to be moved around the plant, thus capable of autonomously navigating within a given map, while avoiding obstacles and ensuring safety for all human operators sharing the same space;
2. a serial *cobot* for local manipulation of objects;
3. a *gripper*, attached to the manipulator end-effector, that performs grasping and pinching operations;
4. a *vision system* (e.g., camera + laser pointer) able to define targets for the cobot in proximity of static elements of the plant, as well as to inspect raw material before loading operations.

Given the objectives and requirements of the use case, the KMR system by Kuka, including a mobile platform (from now on referred to as *AGV*) and a lightweight LBR iiwa 14 manipulator (from now on referred to as *cobot*), was selected (Figure 1c). The main reason behind this choice is the market readiness of the device, together with the convenience of a fully integrated system, which considerably reduces the set-up efforts on the end-user side.

The LBR iiwa has 7 degrees of freedom, which allows targets to be reached in multiple configurations, thus granting a high level of flexibility. Moreover, each joint is equipped with a torque sensor, which grants a quick and safe arrest in case of unexpected contact. The end-effector is equipped with an industrial electrical gripper by Zimmer with custom, inter-changeable fingers, a laser pointer, and an industrial monochrome 2D camera by Matrix Vision. Selection process and details of these solutions are described in Sections 7 and 8.1.

The AGV features Mecanum wheels, which on the one hand make it a holonomic mobile platform, on the other constrain it to a flat horizontal surface, due to slipping tendency on slopes. Numerous on-board sensors ensure a precise and safe navigation within a plant map that can be generated by a preliminary and semi-automatic scanning phase. More safety-related features of this system are discussed in Section 3.

3. Safety

EU directives are European legislative instruments that have the goal of protecting people's health at the workplace. EU directives establish essential safety requirements, while technical standards indicate the recommended solutions to achieve them. Table 2 shows the main standards and directives related to the safety of people working in environments with robots that perform collaborative operations, from the generic to the specific case.

According to ISO/TS 15066:2016, collaborative operations between humans and robots may include one or more of the following safeguarding methods, better described in Bi et al. (2021):

1. safety-related monitored stop;
2. hand guiding;
3. speed and distance monitoring;

Table 2

Main directives and standards for the usage of robots in industry.

Laws & Directives	European Machinery Directive 2006/42/EC
Type A Standards	IEC 61508 - Functional Safety ISO 12100 - Risk Assessment
Type B Standards	ISO 11161 - Integrated Manufactur. Sys. EN ISO 1349-1:2008 IEC 62061:2012
Type C Standards	ISO 10218-1 Robot ISO 10218-2 - Robot System/Cell ISO/TS 15066 - Collaborative Robots

4. power and force limiting.

It is important to note that even if each single robot and other related component satisfies safety requirements, a risk assessment (Matthias and Reisinger, 2016) must be carried out considering the whole application and context.

3.1. Safety Features

Differently from other works, such as the one by Bright et al. Bright, Adali and Bright (2022), where the human-robot collaboration is enhanced by the employment of sensory gloves that can track the hand motion, the main concern in this project is to ensure that whenever a human operator approaches the AMR every component remains still and harmless. Therefore, the strategy adopted here is focused on co-existence rather than direct cooperation between the human and the machine, and, to achieve this goal, commercial devices with built-in safety features are used to guarantee an industry-proof level of safety. Nevertheless, in Sec. 9.1.1 we present the outcome of collision tests that simulate an accidental contact with the human body in the context of our application.

Thanks to the laser scanners located at two opposite corners, the AGV can project a surrounding virtual safety area, also called "protection area", that, when violated, immediately triggers a safety-related monitored stop of the AMR. By enlarging the contour of this area by a fixed offset we have the so-called "warning area", that, when violated, reduces the operational speed of the KMR. These operating speeds correspond to impact forces and pressures that are below the biomechanical thresholds specified in the ISO/TS15066:2016 for the affected body parts. These features are exploited to outline two different safety configurations:

1. **AGV in motion:** when the mobile platform is moving, the manipulator is retracted and idle so that the overall encumbrance of the AMR almost coincides with the AGV footprint, and the size of the safety areas increases proportionally with the AGV speed. In this configuration, the protection area can be set to 300 mm at the maximum speed of 300 mm/s. The value of 300 mm was chosen to ensure the safety for the operators while, at the same time, reducing the frequency of intrusion of obstacles in the protection area when passing through a cluttered and dynamic environment or close to other machines.
2. **AGV stationary:** when the AMR is performing operations that require the motion of the cobot, the AGV is not moving, and the safety areas are suitably designed depending on the task and work position, and set by using the custom safety configuration mode supported by KMR human-machine interface. Due to the short required distance between the KMR and any stationary element, the protection area needs to be cut out so that it does not intersect with the footprint of the stationary element at hand. The trajectories of the cobot are projected on the ground to define, with a suitable margin, a minimum safety boundary on the sides of the AGV not facing the automatic machine or the wagon. The warning area is then built expanding from the outlined protection area while still avoiding the intersection with the machine or wagon footprint. Even if the goal is to stop the manipulator before an operator can accidentally come into contact with it, the high-resolution torque sensors present at each joint of the cobot can still perceive any unexpected contact and rapidly arrest the motion of the arm.

Other measures adopted to enhance safety in the production cell are related to the design of protective casing and additional custom elements on board the AGV, whose edges are rounded in order to increase the accidental contact

surface and reduce the corresponding contact pressure, for a given contact force. Lastly, in order to avoid any risk of trapping and/or crushing for the operator, a minimum space of 500 mm between any fixed structure in the plant and the AMR moving at cruising speed is always maintained.

4. System Architecture and Task Scheduling

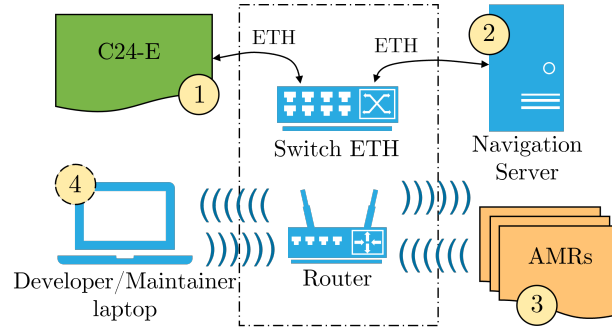


Figure 2: Hardware architecture.

The selection of the architecture of a complex distributed system is a long-discussed topic in the literature of engineering applications (Kim, Park and Kwon (1999), Atta-Konadu, Lang, Zhang and Orban (2005)), and often considers the benefits and drawbacks of a centralized, decoupled or hierarchical architecture. Motion control and many industrial devices often demand real-time capabilities (determinism, timing, etc), but scalability, reconfigurability and other features relevant to the industry world must be taken into account too.

Given the fact that the motion control of the AMR is handled by the onboard KUKA firmware, the only layer that must be integrated is the task scheduling one, for which a hierarchy architecture is selected. This choice is mainly driven by the advantage of being isolated from the actual hardware, and allows abstracting the scheduling problem from the layers below. Moreover, at this level there is no hard real-time constraint, thus, there was no need for resorting to sophisticated architectures or protocols.

Figure 2 summarizes the main blocks composing the architecture of the production cell. From a low-level communication point of view, data are transferred within a LAN, where stationary elements, such as the automatic machine and the navigation server, are connected to a central hub via Ethernet cables, while moving/temporary elements exploit Wi-Fi technology. Each item in Figure 2 is responsible for a particular set of tasks³ illustrated hereafter.

1. **C24-E**: the automatic machine, via MODBUS TCP communication, can invoke the help of an AMR and notifies any change of format and/or machine status.
2. **Navigation server**: the server runs on a stationary workstation, and sorts all pending requests⁴ while monitoring robot fleet status. Moreover it is in charge of managing the plant map as well as the definition of all *work locations*, namely charging stations and static positions close to stationary elements where the AMR performs manipulative operations.
3. **AMR**: each element in the AMR is treated independently, and covers specific tasks:
 - (a) AGV:
 - self-navigation,
 - initial mapping of the plant,
 - safety areas management and monitored stop,
 - enabling the cobot when stationary at a work location;
 - (b) cobot (i.e. manipulator):

³We define as a *task* here a piece of work assigned to an agent, e.g. the AMR.

⁴We define as a *request* here the act of asking for a particular task to be accomplished, formatted in a suitable, computer-friendly way.

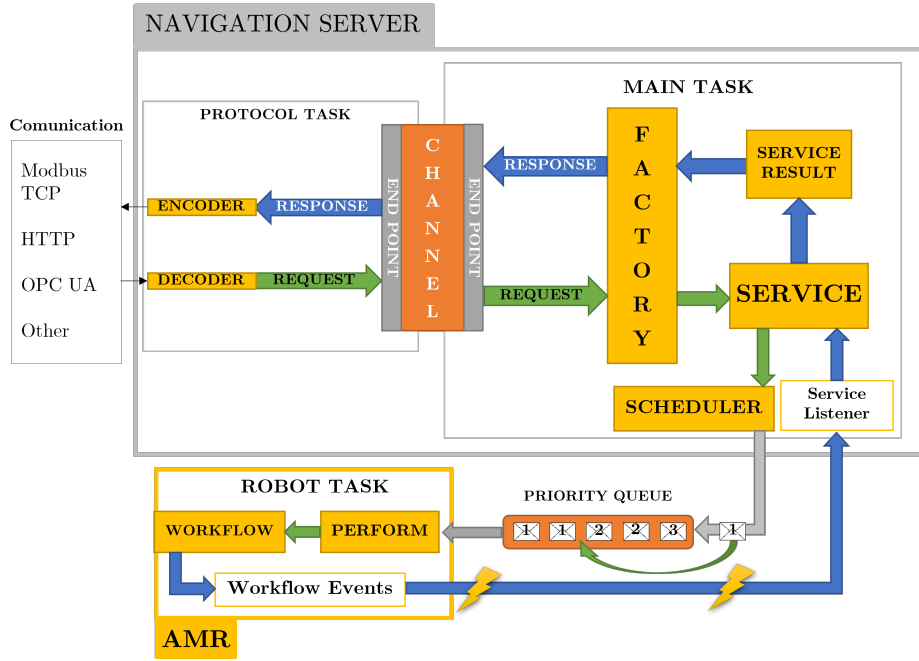


Figure 3: Navigation Server Dataflow.

- trajectory following, i.e. tracking of way-points manually taught by an expert operator and specifically designed for each task,
 - conversion of information received by the navigation server into elementary operations, such as specific object manipulation, positioning, and switching between force and position control mode,
 - gripper operations management,
 - laser pointer management,
 - requests to camera's web server,
 - safety managements in case of unexpected contact;
- (c) camera's web server + vision system:
- scanning of markers applied onto stationary elements for accurate relative positioning of the AMR (see Section 8.2),
 - scanning of blanks to infer stack position,
 - validity check of raw material.

The different communication protocols native of each device that may request a task necessitate a first layer of decoding/encoding on the navigation server' side, which acts as a central control unit for task allocation and request management. With regards to the wireless communication between the navigation server and the AMR, instead, PROFINET is used.

With reference to Figure 3, the *Protocol Task* takes care of decoding an external request, for instance a "Help" request from the automatic machine. The decoded information is passed on to the *Main Task*, and it is used by the *Factory* block to build up a source-independent object, which can be easily interpreted by the system. A *Service* block includes layout and other important information to the object, such as KMR status and charge, and determines which AMRs can handle the pending request. The *Scheduler*, given the available options at disposal and the current task schedules, appends or inserts the new task in the priority queue of each AMR, which locally parses the information and performs the desired operation while providing feedback throughout its execution. The *Service Listener* continuously reads out robot's feedback about its status and the status of the active task to update environmental information.

Eventually, it forwards the results to the *Factory*, that unpacks the response⁵ in a friendly format for the *Protocol Task* to encode it, and to send it back to the origin of the request.

The strong modularity of this architecture makes it protocol independent, and allows each block to be easily replaced, thus leaving room for future improvements and implementation of more sophisticated and better performing blocks. First and foremost the scheduler, currently based on a trivial algorithm due to the limited number of operating AMRs (namely, a single one).

5. Trajectory Planning of the Mobile Robot

5.1. AGV Navigation

The navigation server is the software employed for the management of the AGV navigation. The plant map, together with the laser scanners on-board, allows the self-localization of the AGV.

Once a destination location is assigned within the shop-floor map, the motion planner automatically generates a path, along which the AGV moves, while continuously monitoring the safety areas currently activated. For each safety area, two concentric fields are considered: a warning field and a protection field, where the former is larger than the latter one. When in motion, if the laser system detects an obstacle within the warning area, the AGV reduces its speed and the dimension of the safety area is adjusted accordingly. If the obstacle exits the warning area, the AGV resumes the navigation at the nominal speed. Conversely, if the previously detected obstacle intrudes the protection field, the AGV stops its motion completely.

The SLAM-based autonomous AGV navigation is entirely managed by KUKA proprietary software, whose inputs are represented by a series of target positions, also called work locations, inside the shop-floor map. Hence, the user is only required to accurately determine the work locations for the execution of each specific task, and the navigation system automatically generates the collision-free, shortest path as a series of way-points that connects the target position to the current estimated position in the map.

Self-navigation is often subject to significant drifts that produce error in the final AGV positioning. A *fine positioning* procedure, made available by KUKA software, is thus performed to improve positioning accuracy. Thanks to a 3D matching between the point cloud given by the CAD model of the surrounding scene of the destination and the one obtained by the laser scanner, the position estimate of the AGV on the navigation map is adjusted to minimize the difference with respect to the measured relative offset of the target work location.

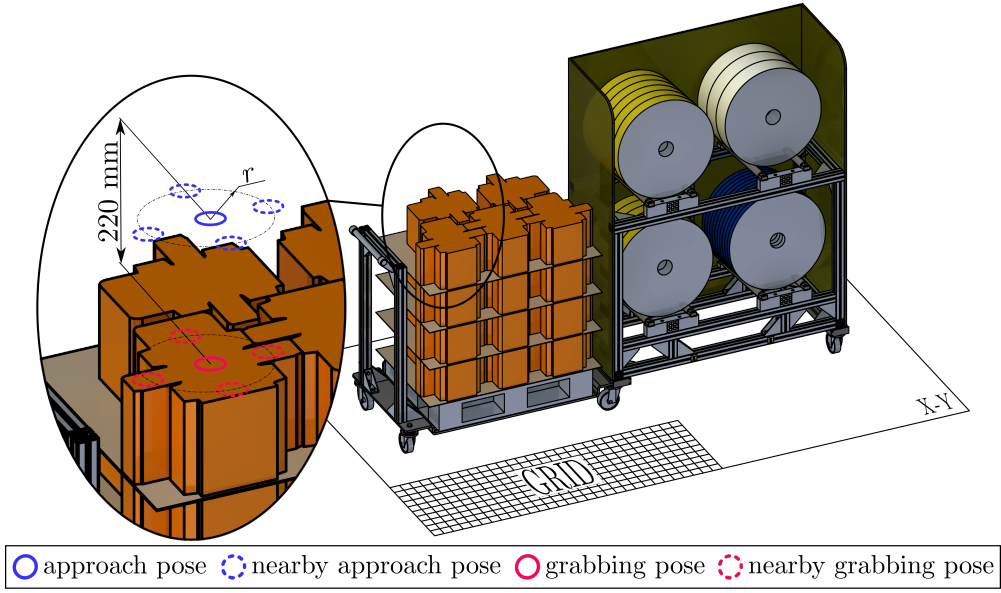
5.2. Optimization of the Work Locations

As far as the reel handling is concerned, the work locations assigned for the trajectory planning of the AGV are determined by manual trials on the shop floor. In particular, only two single work locations in front of the wagon are sufficient to pick up all the reels stocked on the wagon: one for the left reels and one for the right reels. On the contrary, reel loading on the automatic machine requires different locations of the AGV depending on the destination mandrel. The determination of these work locations takes into account the workspace of the cobot w.r.t. the specific reel mandrel, as well as the collision avoidance between the cobot and the mechanical components of the machine.

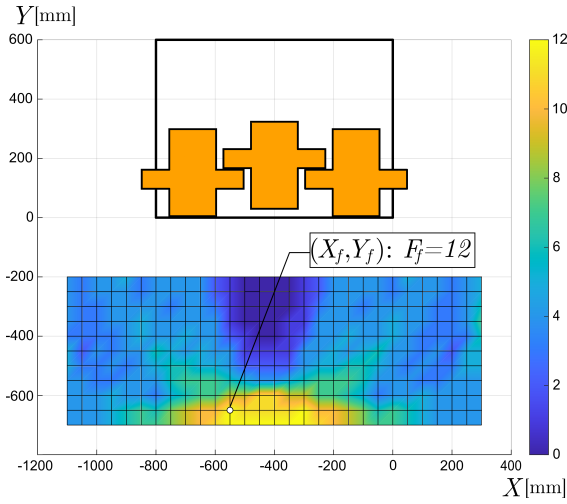
AGV positioning for blank loading on the machine is also determined by manual trials, whereas the choice of work locations for blank depalletizing needs a more accurate analysis.

The accessible area (a rectangle of 500×1400 mm, as shown in Figures 4b and 4c) in front of the pallet is schematized as a $N_X \times N_Y$ grid inside which every element represents a AGV position (X_i, Y_j) , with $i = 1, \dots, N_X, j = 1, \dots, N_Y$ (see Figure 4a, where the example of a pallet composed of 4 layers, each of them hosting 5 blank stacks, is considered). For each position (X_i, Y_j) on the grid, the manipulability of the blank stacks is analyzed. The manipulation of the k -th stack ($k = 1, \dots, N_b$, with N_b being the total number of stacks on the pallet) refers to two different poses of the cobot: the grabbing pose and the approach pose, which is obtained from the first one through an offset of 220 mm along the vertical direction (Figure 4a). Hence, for a given position (X_i, Y_j) of the AGV on the grid, the k -th stack is reachable if and only if the cobot is able to both approach and grab the k -th stack. The optimization of the AGV work locations requires the Inverse Position Analysis (IPA) of the cobot, namely the computation of the joint angles for a desired pose of the cobot end-effector. Since the cobot has 7 degrees of freedom, there are ∞^1 configurations that allow the robot to reach a desired pose. Moreover, for any value assigned to the redundant degree of freedom (in our case, the 4th axis is selected as such), the cobot may assume 8 different valid configurations (namely, solutions of the IPA).

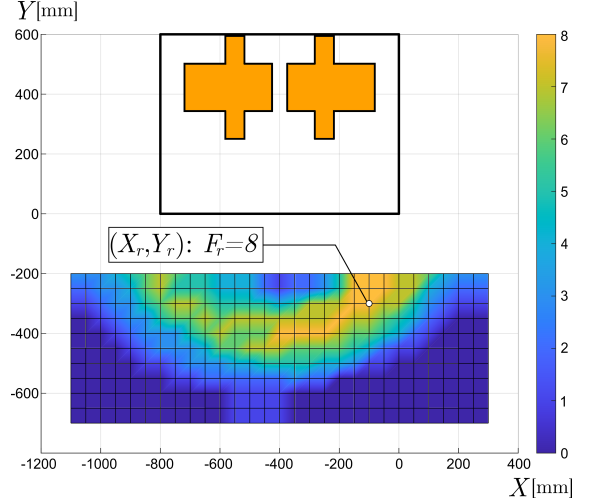
⁵We define as a *response* here a reply given as answer to a task request containing information about the outcome of the performed operation.



(a) Approach, grabbing and nearby poses definition



(b) Work-location choice for the front stack depalletizing



(c) Work-location choice for the rear stack depalletizing

Figure 4: Path planning for the blank depalletizing task of a pallet composed of 4 layers, each of them hosting 5 blank stacks.

For the optimization analysis, each position (X_i, Y_j) is assigned the Feasibility Index F_{ij} . F_{ij} is the number of stacks that can be processed from the (X_i, Y_j) position and from its nearby positions $(X_{i\pm l}, Y_{j\pm l})$, with l being an arbitrary integer value: the higher l , the more restrictive the feasibility request in (X_i, Y_j) . A stack is processable if there is at least one IPA solution and one value of the redundant variable that allow the stack to be correctly handled.

The employment of F_{ij} allows the determination of the optimal position of the AGV from which the cobot is able to process all blank stacks on the pallet. This problem results in finding a position for which the value of the Feasibility Index is equal to N_b . When this condition is not met, the stacks are divided into two groups:

1. the blank stacks placed in the front part of the pallet;
2. the blank stacks placed in the rear part of the pallet.

Thus, the previous problem switches to the research of two optimal positions of the AGV, namely (X_f, Y_f) and (X_r, Y_r) , so that F targets N_{bf} and N_{br} , respectively, where N_{bf}/N_{br} is the total number of the front/rear blank stacks. The formulation of the optimization problem is written in Algorithm 1. The intermediate index $I_{ij,k}$ is a boolean value: $I_{ij,k} = 1$ if the k -th stack is reachable from all the AGV positions (X_i, Y_j) and $(X_{i\pm l}, Y_{j\pm l})$, $I_{ij,k} = 0$ otherwise.

Algorithm 1 Algorithm describing the workflow for the optimization of the AGV work locations.

```

1: procedure OPTIMIZATION
2:   Solve  $\max_{\substack{i=1,\dots,N_X \\ j=1,\dots,N_Y}} F_{ij}$ , where  $F_{ij} = \sum_{k=1}^{N_b} I_{ij,k}$ 
3:   if  $(i^*, j^*) | F_{i^*j^*} = N_b$  then
4:      $(X_{i^*}, Y_{j^*})$  is the optimal AGV location
5:   else
6:     Solve  $\max_{\substack{i=1,\dots,N_X \\ j=1,\dots,N_Y}} F_{ij}$ , where  $F_{ij} = \sum_{k=1}^{N_{bf}} I_{ij,k}$ 
7:     if  $(i^f, j^f) | F_{i^fj^f} = N_{bf}$  then
8:        $(X_f, Y_f) = (X_{i^f}, Y_{j^f})$  is the optimal AGV location for the front stacks
9:     end if
10:    Solve  $\max_{\substack{i=1,\dots,N_X \\ j=1,\dots,N_Y}} F_{ij}$ , where  $F_{ij} = \sum_{k=1}^{N_{br}} I_{ij,k}$ 
11:    if  $(i^r, j^r) | F_{i^rj^r} = N_{br}$  then
12:       $(X_r, Y_r) = (X_{i^r}, Y_{j^r})$  is the optimal AGV location for the rear stacks
13:    end if
14:  end if
15: end procedure
    
```

The choice of the optimal AGV positions is represented in Figure 4b for the front blanks, where the feasibility index in correspondence of (X_f, Y_f) is indicated as F_f and its value targets $N_{bf} = 12$, and in Figure 4c for the rear ones, where F_r is the value of the feasibility index in the optimal work location (X_r, Y_r) and is equal to $N_{br} = 8$.

5.3. Cobot Trajectory Choice

Once the AGV positioning optimization is solved, the blank-depalletizing task requires a further analysis step: given the position (X_f, Y_f) or (X_r, Y_r) , the cobot IPA configuration and the redundant-variable value (namely, the 4th-axis angular variable) still needs to be chosen. To obtain a more robust result, the existence of an IPA solution is sought, not only in correspondence of the approach and grabbing poses, but also in their neighborhoods. In particular, for each of the two poses, with a fixed orientation, the IPA is solved also in 4 equi-spaced points located on a circle, which lies on a plane parallel to the $X - Y$ plane and whose radius is equal to r (Figure 4a). The procedure is as follows:

1. for each blank stack, the solutions relative to the approach and grabbing poses, and their nearby positions, are considered in terms of feasible redundancy ranges⁶; 10 redundancy intervals are then obtained for each IPA solution;
2. taken the i -th IPA solution ($i = 1, \dots, 8$), the intersection of the 10 intervals gives the i -th feasibility interval/s;
3. among the 8 IPA solutions, the one which is characterized by the largest redundancy interval is chosen, and the redundant-variable value is calculated as the mean of the selected range;
4. the outputs of the analysis are fed to the cobot controller for the manipulation of the k -th blank stack.

⁶For each desired pose, the redundant variable is assigned a value within the discretized interval $[-\pi, \pi]$. In correspondence of each value of the discretized interval, the IPA is solved considering the other 6 joint angles: if a solution exists, that value of the redundant-variable belongs to the feasible redundancy range.



Figure 5: Snap-shots of a reel feeding task.

6. Manipulation Strategies for the Cobot

The manipulation strategies adopted for the cobot can be distinguished into two main tasks: reel feeding and blank feeding. While the former one involves the final intervention of an operator given the human-level dexterity required for the last part of the task, the latter one is completely machine-driven. Recovery procedures from a possible failure at any stage of both tasks are described in Section 6.3.

6.1. Reel Feeding⁷

The reel feeding task considers the following workflow.

6.1.1. Preliminary Actions

When a specific reel has ran out, the C24-E control unit commands some preliminary automatic operations on the machine: the reel mandrel rotates until all remaining material is rewound on the core, and the radial supports on the mandrel, which grasp the reel from the inside, are released. Once these operations are completed, the C24-E control unit communicates to the navigation server that the machine is ready, and the latter proceeds with the choice of an available AMR to handle the reel-feeding request.

6.1.2. Reel Picking

The AGV navigates until it approaches the wagon with fine positioning. Then, the following operations are executed:

- (a) *Reel scanning*: once the AGV is correctly placed, the cobot detects the marker that determines the pose from which it can start scanning the desired reel. Thanks to the laser pointer mounted on the end-effector, the cobot detects the core diameter and its centre point position. Once the pose of the reel is known, the cobot adjusts its configuration and, thanks to a further scanning, it finds the offset along the z-direction of the end-effector that has to be covered to begin the grasping of the reel.
- (b) *Reel grasping*: once the grabbing pose is reached, the gripper opens its fingers under position control mode, in order to grasp the reel from inside the core.
- (c) *Reel buffering*: the cobot stores the reel on a designated support aboard the AGV and the control unit saves the reel deposit pose for the next manipulations. Before the cobot returns to the home configuration, a photocell checks whether the reel has been correctly stored.

6.1.3. Core Removal

The navigation server sends to the AGV the specific work location of the reel that has to be loaded on the machine. After completing the fine positioning of the AGV, the following procedures are executed:

- (a) *Marker detection*: the cobot reaches a pose that allows it to detect the mandrel pose, which is saved by the control unit (see Section 8.2).

⁷The reel-feeding task is shown in the attached video *reel_loading.mp4*.

- (b) *Core grasping*: the cobot aligns its end-effector with the mandrel and commands the gripper to open; an offset translation is then needed to align the fingers to the core, and the fingers close under force control to grasp the core from the outside.
- (c) *Core disposal*: the cobot extracts the core and deposits it in a container aboard the AGV.

Since the tag-reel core diameter exceeds the stroke that can be covered by the gripper, its removal requires a different strategy. The mandrel that hosts the tag reel is equipped with a mobile sliding body. The cobot grasps the mandrel "nose" and makes the mobile body push the core out along the mandrel. Then the gripper may grab the core from the inside and deposit it⁸.

6.1.4. Reel Loading

- (a) *Reel grasping*: thanks to the previously saved deposit pose, the cobot is able to quickly move towards the reel stored in the on-board buffer. By using torque sensors, the cobot detects when the contact between the gripper fingers and the reel occurs: the cobot retracts 10 mm, opens the fingers under position control, and grasps the reel from the inside of its core.
- (b) *Mandrel approach*: the cobot grabs the reel from the buffer, and moves it until it aligns with the mandrel pose saved during the mandrel marker detection.
- (c) *Reel loading*: under force and impedance control mode, the cobot moves forward along the end-effector z-direction in order to fit the reel onto the mandrel. This control mode allows to compensate for possible misalignment between the reel axis and the mandrel axis. The cobot partially closes the gripper fingers until they enter in contact with the mandrel nose, then retracts, hence disengaging the reel, and begins the pushing phase: after opening the fingers to the maximum stroke, the cobot pushes the reel along the mandrel axis direction until the reel is correctly placed. Once the task is accomplished, the cobot returns to its home configuration and the radial supports are activated to block the reel on the mandrel.

The operations regarding the reel grasping and the pushing phase are shown in Figure 5. When the task is complete, a human operator's attention is called to the automatic machine to indicate that the reel is loaded and ready for the *splicing* preparation. This job consists in unwinding the first strip of the reel and passing it through rollers and clamps. When finished, the automatic machine is able to automatically splice the strips from two different reels of the same type, so that the production is never interrupted.

6.2. Blank Feeding⁹

6.2.1. Stack Picking

According to the blank stack that has to be processed, the navigation server knows in which work location in front of the pallet the AGV has to position itself for the manipulation. The operation flow is as follows:

- (a) *AGV fine positioning*: the AGV finely positions itself in the work location, with the same procedure described in Section 6.1.2.
- (b) *Stack detection*: the vision system mounted on the cobot end-effector takes a photo of the printed side (hereafter referred to as 'texture') on the stack. By image processing, the pose of the stack is determined. For more details, see Section 8.4.
- (c) *Stack picking*: knowing the geometry of the stack and its pose, the cobot reaches the approach pose and then, by a translation along the end-effector z-axis, the grabbing pose. By exploiting the particular shape of the stack (Section 7.1.2), the cobot executes the grasping task.
- (d) *Stack overturning*: while the blanks are placed on the pallet with the texture pointing upward, they have to be loaded on the automatic machine with the texture pointing in the opposite direction. For this reason, the stack must be flipped by resorting to a customized buffer mounted on the AGV (Section 7.2).

Once the overturning operation is finished, the cobot maintains its last pose (with the gripper still grasping the stack) in order to prevent the stack from falling apart or down during the navigation towards the blank-loading work location.

⁸This procedure is shown in the attached video *tag_reel_core_removal.mp4*.

⁹The blank-feeding task is shown in the attached video *blank_feeding.mp4*.

6.2.2. Stack Loading

After a fine positioning of the AGV on the blank-loading work location, two main operations are performed:

- (a) *Marker detection*: while holding the stack, the cobot detects the marker of the loading buffer of the automatic machine, by using its eye-on-hand camera.
- (b) *Stack loading*: after the marker detection, the cobot computes the loading pose that it has to reach for blank loading. Finally, the cobot moves the stack and loads it on the machine.

6.3. Failure Management

There are in total 5 failures that trigger, as a first step, a dedicated automatic fall-back operation¹⁰. For example, if a marker is not detected, the cobot tries up to five times to re-perform the detection by applying small changes to the original framing pose before taking a new shot, thus reducing any systematic error. If that fails too, the MRU moves back to the charge station and an alarm signal is emitted to draw the operator attention. The same fall-back operation is carried out upon the detection of a missing reel. This is done utilizing the laser pointer on the end-effector before the picking phase near the wagon. Similarly, a dedicated photo-cell pointing at the reel buffer on board is used to perform this safety check before the loading phase near the automatic machine.

In case of hard fault or more serious errors that require human intervention, supervised semi-automatic recovery procedures are available through the touch-pad of the KMR to restore the correct functioning of the system, such as:

1. restoring without reel attached;
2. restoring with reel attached;
3. gripper manual opening/closing;
4. gripper homing;
5. force sensor zeroing;
6. cobot brakes test.

7. Mechanical Design of Custom Components

The different shapes of the objects to be manipulated by the robotic system require some customized components to be manufactured.

7.1. Custom Gripper Fingers

The initial idea was to build a universal gripper from scratch, capable of processing both the reels and the blanks. However, because of its complexity and bulky size, this solution was finally discarded. Hence, the final design of the gripper follows two different paths, according to the objects to manipulate.

7.1.1. Reels

As shown in Figure 6a, two different pairs of fingers are employed for reel processing. The first one is able to process both the filter paper and the outer-envelope reels. The round shape of the fingers fits the inner curvature of the reel core in order to ensure a firm grip of the object. The second type of fingers is designed for grabbing tag reels. The only difference is the addition of lateral wings, which prevent the so-called 'streamer effect': an undesired unwinding of the reel during the manipulation, due to the sliding of adjacent layers.

7.1.2. Blanks

The triangular prisms fill the blank interstices (Figure 6a), and help to firmly grab the stack. A flexible spatula at the end of each finger is employed to make sure that the whole stack is picked up, while the upper blade prevents the stack from excessively bending during the overturning phase. In Figure 6a, the spatula of the right blank finger has been hidden from the CAD model for the sake of clarity.

¹⁰ An operation that reverts a failed change of state and brings the system back to the original one.

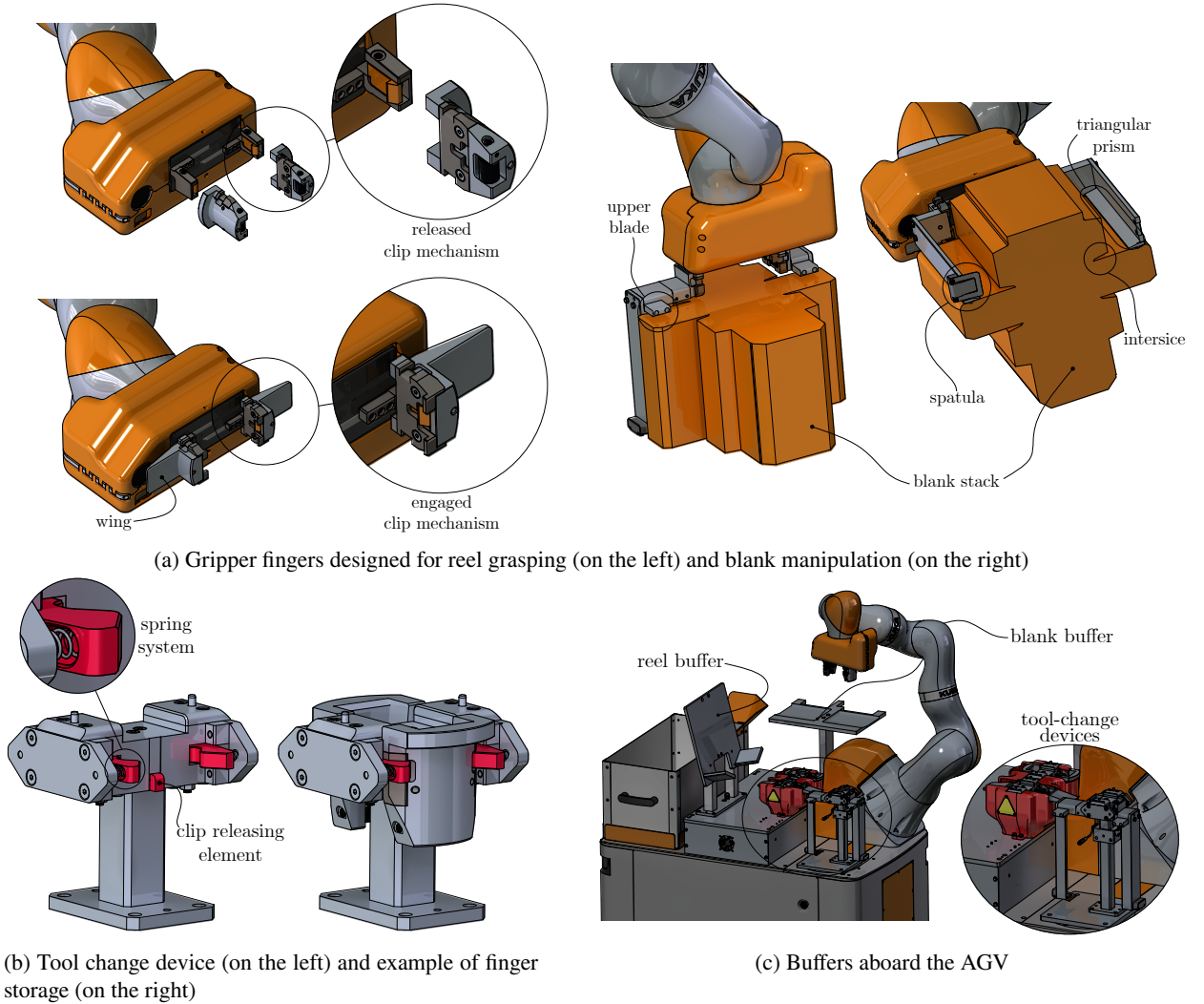


Figure 6: Custom mechanical components.

7.1.3. Tool Change¹¹

Each finger is designed to allow automatic tool changeover. Tailored mechanical devices mounted on the AGV (one for each finger type - see Figure 6c), thanks to a tooth-shape spring system, are used to release the clip mechanism that connects the finger to the gripper, detach the fingers and store them until the next changeover (Figure 6b).

7.2. AGV Buffers

In order to handle the objects (reels/blanks) aboard the AGV, storing devices are needed. In particular, for the reel buffer, a simple plate with two oriented supports allows reels with different diameters to be hosted. On the other hand, the blank buffer mounted on the AGV not only hosts the stack, but it also helps the flipping operation, thanks to the tailored profile of the plate. Both buffers are shown in Figure 6c.

8. Computer-Vision-Based Tools and Solutions

While sensors available on the AGV ensure safety when roaming on the shop-floor, a short-range high-resolution device is employed to collect non-safety-related information to be used for high-level motion planning and for interaction with the environment (e.g. the automatic machine and the wagon). For this purpose, an industrial camera

¹¹The tool-change operation is shown in the attached video *tool_change.mp4*.

is selected due to its relatively low cost and large amount of information it can deliver, which leads to a high level of flexibility and re-usability.

8.1. Mono vs Stereo Vision

The main goals of the vision system are delivering accurate relative position and orientation of the stationary elements of the plant with respect to the coordinate system of the cobot, and identifying the pose of the blanks lying on the wagon while checking their validity. In particular, the former need arises from the pose uncertainty of the AGV upon reaching target location in the plant. In fact, both the pick-up phase of the reels from the wagon and the loading phase on the automatic machine require a millimeter accuracy, which we were not able to attain with the integrated navigation system of the AGV. To this end, two solutions were considered:

1. a *stereo-camera* mounted on a pan-tilt unit installed on the top surface of the AGV, next to the cobot; thanks to binocular vision, this sensor is able to directly capture 3D images, thus estimating the pose of objects from a point cloud generated from a single pair of corresponding frames;
2. a *mono-camera* mounted on the end-effector of the cobot (i.e. *eye-on-hand* configuration) and the application of visual markers on predetermined positions suitably located on the work locations; by exploiting the markers, it is possible to estimate their poses from single images given the camera projection model obtained from calibration.

Both solutions share the same advantages, such as easy-installation and good speed and spatial resolution. On the other hand, preliminary tests showed a poor performance of the former one, mainly due to the limitation given by its fixed position on the mobile platform. The framed objects were, in fact, often out of focus because of the different operational distances required by the task, or even out of frame due to the narrow attainable field of view. Moreover, the presence of such unit on the AGV imposed strong constraints on the cobot motions, thus reducing its workspace. The eye-on-hand solution is, instead, more flexible and can handle a larger number of operations, including the blank-pose identification, which is more challenging via a single stationary pan-tilt unit. On the other hand, this solution requires the adoption of specific markers suitably distributed in the plant, as discussed in Section 8.2.

8.2. Marker Detection

The detection of a marker board is an important step in our application as it is used both in the calibration procedure described in Section 8.3, and in the relative positioning of the AMR with respect to stationary plant elements.

A *ChArUco board*, namely a combination of a chessboard pattern and an ArUco board, is chosen as marker type as it benefits from both approaches. On the one hand, a chessboard allows a very accurate pose estimation due to the precise detection of many corners. On the other hand, it needs to be fully visible in an image, thus, being subject to failure in case of partial occlusion. Conversely, an ArUco board contains many ArUco markers, which allows a very fast board detection even if some markers are occluded. Even if the estimated pose is not optimal due to the low accuracy of detected corners, it can be used to interpolate the position of the missing chessboard corners, leading to a complete, improved result. Nonetheless, attention must be paid to the size of the board, because it needs to be big enough to allow the detection of the markers, but small enough for a suitable installation. Markers employed in this application are displayed in Fig. 7.

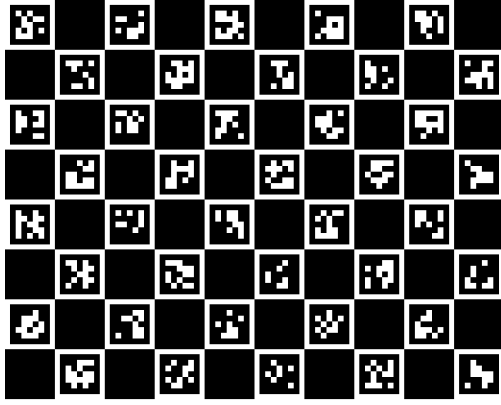
Standard functions from OpenCV library (Bradski, 2000) are used to estimate the board poses with respect to the camera frame. Repeatability errors were calculated to be in the order of 0.01 mm for position and 0.01° for orientation.

8.3. Calibration

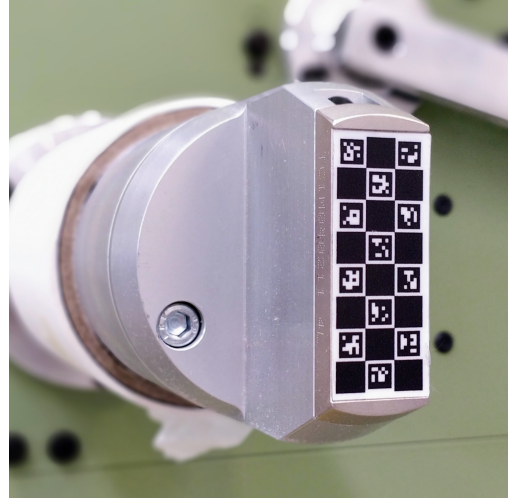
A repeatable calibration procedure is required to exploit the captured visual information and convert them into useful data in robot coordinates. To this purpose, the well-known pin-hole model with radial distortion correction is considered for the estimation of the intrinsic parameters of the camera and a common pattern-based calibration is performed leveraging OpenCV utilities based on Zhang (2000).

As far as the extrinsic parameters are concerned, that is the coordinate transformation between the camera frame and, in the eye-on-hand configuration case, the end-effector frame, a robot-independent neural-network-based approach is implemented.

The calibration pattern is placed on a flat surface close to the manipulator and the camera is moved so as to frame the board from different N perspectives. At each step $i = 1, \dots, N$, the TCP pose expressed in robot's coordinates ${}^{rob}\mathbf{p}_{tcp,i}$ is registered together with the board pose estimate with respect to the camera ${}^{cam}\mathbf{p}_{board,i}$, obtained from marker detection through image processing.



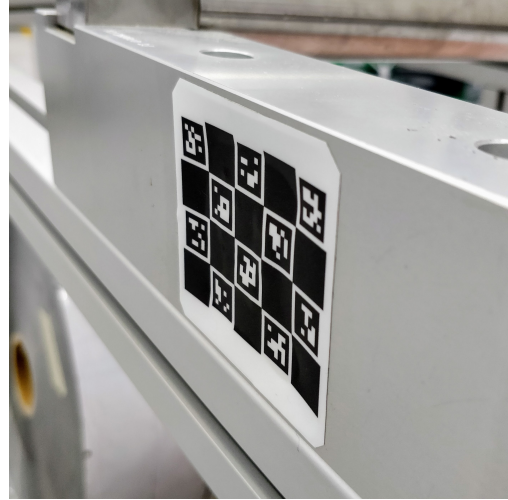
(a) 10x8 calibration pattern



(b) Paper filter/outer envelope reel mandrel 3x8 marker



(c) Tag reel mandrel 5x4 marker



(d) Wagon shelf 5x4 marker

Figure 7: ChArUco boards employed.

A shallow neural network is trained to minimize the L2 loss (i.e. mean squared error) between the measured ${}^{rob}\mathbf{p}_{tcp,i}$ and the re-projected ${}^{rob}\hat{\mathbf{p}}_{tcp,i}$ obtained from the kinematic loop closure using ${}^{cam}\mathbf{p}_{board,i}$. *Keras*, a high-level wrapper for *TensorFlow*, the machine learning library from Google, is used to solve this problem, and is employed to define a single network layer that takes care of this computation. Moreover, a simple outlier detection function is implemented to remove samples that may worsen the results, and the training is repeated until results are satisfactory.

The laser pointer mounted besides the camera on the cobot wrist was used to test the accuracy of calibration. After the pose estimation of a known ChArUco board, the laser is moved so that it points at the origin of the detected marker reference frame, with the beam aligned with its Z -axis. Next, a translation along both the estimated $+X$ -axis and $+Y$ -axis is performed, and the drift between the ideal and true path is measured to infer error on the position and orientation. Experimental results showed errors smaller than 1 mm on the position and smaller than 0.1° on the orientation.

8.4. Blank Identification

Exploiting the highly descriptive texture on the blanks and the unique shape of their silhouette, common feature/template matching techniques from computer vision and OpenCV are employed. Not only the detection gives

the accurate location of each single stack, but also provides a way to check whether the type of blank coincides with the expected one, triggering a warning otherwise.

Once the blank pattern is identified, by leveraging the knowledge of the true dimensions of the stack, the camera model, and the results of the eye-on-hand calibration, it is possible to send suitable target points to the cobot's controller to execute the grasp (see Section 6.2).

9. Validation and Prospectives

9.1. Field Experiments at IMA

The robotic system has been extensively tested at IMA's facilities before its installation at the client production line. During tests, standard working conditions were simulated, to prove the effectiveness of the robotic solution in two different scenarios.

9.1.1. Shared working area

Once a raw-material request was sent to the navigation server through the human-robot interface, the AMR safety assessment was performed. In particular, during the mission accomplishment, the AGV safety areas were often violated on purpose to verify whether the AMR effectively stopped its operations (both during AGV navigation and cobot manipulation), and resumed them once the safety areas were cleared. Additionally, the impact force, which the cobot was able to exert in case of a collision with the components of the AM, was tested. The tests concerning the impact force were conducted in order to simulate circumstances in which the presence of the operator could be intercepted by the cobot manipulative tasks, but could not be detected by the AGV laser scanners. This could occur for the following tasks:

1. the tag-reel core removal, during which the sequence needed to pull the mandrel nose or to extract the core could cause crushing of the operator's fingers;
2. the outer-envelope reel loading, during which the cobot could enter in contact with the operator's legs or abdomen.

The impact and clamping force values were determined by using a GTE KMG 500 measuring system and pressure images generated on Fuji-Prescale films. Such values were then compared with the thresholds dictated by the ISO/TS 15066:2016 standard. At the first attempt, the measured forces exceeded the admissible values. For this reason, two different precautions were applied:

1. during the tag-reel core removal, the cobot force-sensor threshold was decreased, in order to interrupt the cobot motion before reaching an unacceptable impact force for the operator's safety;
2. since the outer-envelope reel loading requires the manipulation of heavy objects, hence excluding the possibility of decreasing the cobot force-sensor threshold, the only feasible action was the reduction of the cobot end-effector velocity, which ensured an admissible impact force in case of a collision with the operator.

9.1.2. Clear working area

Experiments were conducted on all three reel types, for a total of 265 tests. The latter resulted in 259 successful operations, thus demonstrating the reliability of the proposed robotic solution. As far as the 6 faults are concerned, 2 of them were caused by the impossibility to reach the farthest reels on the wagon, 3 faults were due to an incorrect AGV positioning, whereas 1 fault was related to tag-reel ovalization due to an excessive force exerted by the gripper. For the first and second fault types, two mechanical modifications were performed: the reel support plate was relocated on the wagon, and the lower parts of the wagon and the automatic machine were redesigned by adding a custom profile that improves the AGV fine-positioning procedure. In order to mitigate the ovalization problem, hybrid position-force control was implemented in grabbing the reel.

9.2. Client Feedback

The robotic system was also tested at IMA's client factory, where the first 97 attempts obtained a percentage of success equal to 76.3%. Among the different failures, 10 were caused by an AGV positioning error, due to which the vision system could not operate a proper marker detection; 6 were due to an emergency stop triggered by the operator,

Table 3
Task time optimization.

Reel type	T_b [min:sec]	T_a [min:sec]	Saved time [%]
Right filter-paper	04:57	02:57	40,40
Left filter-paper	05:08	02:57	42,53
Right tag	06:06	02:59	51,09
Left tag	05:32	03:01	45,48
Right outer-envelope	06:07	03:29	43,05
Left outer-envelope	06:22	03:11	50,00

as a result of an inaccurate reel buffering, loading or manipulation; 3 were due to a bug in the control code; 2 were the direct consequence of a sudden emergency stop after which the AGV lost information about its location; the last 2 were produced by an AGV localization loss, which pushed the AGV away from the planned path, causing an emergency stop.

While the bug in the control code was fixed, other possible failure avoidance strategies were identified: the addition of custom profiles (as those mentioned in Section 9.1) within the client's production line could improve the AGV fine positioning, hence reducing the risk of undetected markers. The AGV localization problems could also be mitigated by planning periodic re-mapping of the plant. However, this solution is time-consuming, and it would need to be executed every time a slight or an accidental re-positioning of wagons, pallets, or toolboxes is operated inside the working area of the AGV. While the experimental plant at IMA's facilities was always in order and free from external disturbances, the client's factory was often subject to rearrangements. The outlined strategies to increase the robustness¹² of the system, hence leading to a higher percentage rate of success at the client production line, are currently the object of further analysis and implementation.

9.3. Task-Execution Time Reduction

As shown in Sections 5, 6, the complete automation of the material feeding tasks requires a series of routines to guarantee the success of the operations, as well as preventive measures (e.g. the adjustment of the AGV speed according to the activated safety areas) to ensure the collaborative feature of the task execution. The time-consuming characteristics of these (necessary) actions have a high impact on the total time spent to accomplish a single task, thus requiring a number of AMRs, capable of feeding the whole production line, which may exceed the expectations of a possible buyer. For this reason, some improvements can be introduced. In particular:

1. the current cobot manipulation paths, which are defined by means of piece-wise line segments connecting the trajectory endpoints, can be conveniently smoothened; this adjustment will result in a more fluent motion, thus allowing end-effector velocities up to 900 mm/s, instead of the actual velocity of 300 mm/s;
2. the AGV speed velocity may be increased from 100 mm/s to 300 mm/s while employing custom safety areas specially designed to avoid unnecessary AGV stops due to static obstacle detection on the plant map;
3. the automatic tool-change operation could be executed in idle time during the AGV navigation from a work location to another, with the cobot trajectories still remaining inside the AGV boundaries.

While the first improvement on the cobot trajectories can be easily implemented, the last two adjustments still represent an open topic that needs a further risk assessment. If safety proves not to be compromised by this optimization, a time reduction of almost 40 – 50% w.r.t. the previous arrangement could be achieved (as shown in Table 3). In particular, Table 3 compares the execution time T_b spent by the robotic system to accomplish the reel loading operations, without the application of the optimized features, and the execution time T_a of the same robotic system after the optimization. The percentage saved time is calculated as $(T_b - T_a)/T_b\%$.

¹²Robustness is intended here as a measure of the insensitivity of the AMR to disturbances when in operation.

An additional source of slowness on the field is represented by the occasional stop/resume cycles of the AMR when an unexpected obstacle appears too close. Dynamic obstacle avoidance¹³ on both AGV (Weckx, Vandewal, Rademakers, Janssen, Geebelen, Wan, Geest, Perik, Gillis, Swevers and van Nunen, 2020) and manipulator (Dumontel, Manfredi, Devy, Confetti and Sidobre, 2015) sides could prevent undesired downtimes, and, thus, make the robotic system more saleable on the market. This topic is currently under investigation.

9.4. Towards the future: the ROSSINI project

In 2018, IMA joined the consortium of the Rossini EU project¹⁴. The project target is to design, develop and demonstrate a modular, scalable and resilient platform for the integration of human-centered robotic technologies in industrial production environments. *Resilience* is a recent property of productive systems which is now one of the main drives of many projects, especially within the European Union. In Zhang and van Luttervelt (2011), Zhang and van Luttervelt present an accurate analysis of the subject and introduce the concept of *Resilient Manufacturing System* (RMS). They also provide generic and general guidelines that may orient the developers towards the design of new RMSs by birth. Despite the fact that the presented robotic system inherently already tracks guidelines I and II (i.e., redundancy and total function), within the scope of ROSSINI, IMA contributes with a use case that evolves from the MaXima project described in this article to an even more resilient system.

A new AMR is being designed by integrating a MiR500 AGV by Mobile Industrial Robots A/S and two UR10e by Universal Robots. The dual-arm configuration aims at speeding up the execution time of most tasks by parallelization and increasing the maximum payload that can be manipulated. While one manipulator mounts the same tools described in Sections 7.1 and 8.1, the second robotic arm is equipped with a 3-finger gripper by Robotiq that allows finer and adaptive grasping for more sophisticated operations. Moreover, the new hardware allows an easier transition to ROS (Robot Operating System) to control all elements of the new robotic system, as well as to communicate with the external technologies developed by other parties of the consortium.

Further improvements, already at a testing phase, include:

1. the employment of only image processing to determine the reel-core pose, without resorting to a laser pointer; on top of removing a redundant sensor, this strategy should lead to a faster detection;
2. the implementation of a faster routine for automatic eye-on-hand camera calibration on board, based on the work by Tsai and Lenz (1989).

10. Conclusions

In this article we presented a robotic system that is able to perform autonomous cycles of raw-material loading on a tea-packaging automatic machine in an environment safely shared with human operators. Starting from industrial solutions available on the market, a pre-integrated mobile robot composed of an AGV and a redundant serial cobot was selected and equipped with additional sensors and devices tailored to the project goals, such as a custom gripper allowing automatic tool change for the manipulation of different types of objects, namely reels and cardboard blanks. The modular architecture of the communication and decision-making softwares makes the system easy to maintain and extend, and provides an easy link to pre-existent automatic machines that can be served by the robot. Suitable computer-vision strategies were employed to produce reliable and robust trajectory targets for raw-material manipulation and for interfacing with stationary elements of the robotized production cell. Moreover, feature-matching algorithms were used to assess the validity of the manipulated objects.

Despite the promising results achieved during the experimental phases, the moderate success rate (76%) showed in the field tests at the client's factory proved the need for further enhancements to bring the product to its full potential. In particular, increasing the robustness and the task-execution speed are the next goals to achieve the expected marketability and profitability of the proposed solution. Besides that, the collaborative features of the system already allow its integration in pre-established factory layouts with little adjustments and no need for protective fences. Moreover, optimizations at various levels already provide competitive task-execution times that may justify the investment and improve the productivity in a tea-packaging plant, as well as the life quality of the human operators working therein.

¹³The capability of instantaneously re-planning a new collision-free path whenever an unexpected obstacle appears.

¹⁴ROSSINI - *RO*bot enhanced *Se*nSing, *IN*telligence actuation to *Im*prove job quality in manufacturing, Oct. 2018, Grant Agreement Number 818087.

Acknowledgment

The authors would like to thank: the Institute of Robotics of the Johannes Kepler University Linz for their help in the preliminary stereo-vision setup mentioned in Section 8.1, and the ChArUco-marker usage described in Section 8.2; and the IRIS Lab of the University of Aveiro for their help in the blank identification described in Section 8.4.

Furthermore, the support of the Italian Ministry of Economic Development is gratefully acknowledged for partially funding the MaXima project (Decree 15/10/14, CUP B73D15001070).

References

- , 2018. Advanced industrial robotics: taking human-robot collaboration to the next level. Technical Report. European Foundation for the Improvement of Living and Working Conditions. URL: <https://www.eurofound.europa.eu/sites/default/files/wpfomeef18003.pdf>.
- Atta-Konadu, R., Lang, S., Zhang, C., Orban, P., 2005. Design of a robot control architecture, in: IEEE International Conference Mechatronics and Automation, 2005, pp. 1363–1368 Vol. 3. doi:10.1109/ICMA.2005.1626752.
- Berntorp, K., Arzen, K.E., Robertsson, A., 2012. Mobile manipulation with a kinematically redundant manipulator for a pick-and-place scenario, in: 2012 IEEE International Conference on Control Applications, IEEE, Dubrovnik, Croatia. pp. 1596–1602. doi:<https://doi.org/10.1109/CCA.2012.6402361>.
- Bi, Z., Luo, C., Miao, Z., Zhang, B., Zhang, W., Wang, L., 2021. Safety assurance mechanisms of collaborative robotic systems in manufacturing. Robotics and Computer-Integrated Manufacturing 67, 102022. URL: <https://www.sciencedirect.com/science/article/pii/S0736584520302337>, doi:<https://doi.org/10.1016/j.rcim.2020.102022>.
- Bortolini, M., Ferrari, E., Gamberi, M., Pilati, F., Faccio, M., 2017. Assembly system design in the industry 4.0 era: a general framework. IFAC-PapersOnLine 50, 5700–5705. URL: <http://www.sciencedirect.com/science/article/pii/S2405896317316117>, doi:10.1016/j.ifacol.2017.08.1121.
- Bradski, G., 2000. The OpenCV Library. Dr. Dobb's Journal of Software Tools .
- Bright, T., Adali, S., Bright, G., 2022. Low-cost sensory glove for human-robot collaboration in advanced manufacturing systems. Robotics 11. URL: <https://www.mdpi.com/2218-6581/11/3/56>, doi:10.3390/robotics11030056.
- Dumonteil, G., Manfredi, G., Devy, M., Confetti, A., Sidobre, D., 2015. Reactive planning on a collaborative robot for industrial applications, in: Proceedings of the 12th International Conference on Informatics in Control, Automation and Robotics - Volume 2: ICINCO., INSTICC. SciTePress. pp. 450–457. doi:10.5220/0005575804500457.
- Dömel, A., Kriegel, S., Kassecker, M., Brucker, M., Bodenmüller, T., Suppa, M., 2017. Toward fully autonomous mobile manipulation for industrial environments. International Journal of Advanced Robotic Systems 14. doi:10.1177/1729881417718588.
- Iriondo, A., Lazkano, E., Susperregi, L., Uraín, J., Fernandez, A., Molina, J., 2019. Pick and place operations in logistics using a mobile manipulator controlled with deep reinforcement learning. Applied Sciences 9, 348. doi:10.3390/app9020348.
- Kim, Y.S., Park, H.S., Kwon, W.H., 1999. An architecture for a network based robot control system, in: 1999 7th IEEE International Conference on Emerging Technologies and Factory Automation. Proceedings ETFA '99 (Cat. No.99TH8467), pp. 875–880 vol.2. doi:10.1109/ETFA.1999.813084.
- Krug, R., Stoyanov, T., Tincani, V., Andreasson, H., Mosberger, R., Fantoni, G., Lilienthal, A.J., 2016. The next step in robot commissioning: Autonomous picking and palletizing. IEEE Robotics and Automation Letters 1, 546–553. doi:10.1109/LRA.2016.2519944.
- Magnavita, N., 2017. Productive aging, work engagement and participation of older workers. a triadic approach to health and safety in the workplace. Epidemiology, Biostatistics and Public Health 14.
- Matthias, B., Reisinger, T., 2016. Example application of iso/ts 15066 to a collaborative assembly scenario, in: Proceedings of ISR 2016: 47st International Symposium on Robotics, Munich, Germany. pp. 1–5.
- Michalos, G., Makris, S., Spiliotopoulos, J., Misios, I., Tsarouchi, P., Chrysosouris, G., 2014. ROBO-PARTNER: Seamless human-robot cooperation for intelligent, flexible and safe operations in the assembly factories of the future. Procedia CIRP 23, 71–76. URL: <http://www.sciencedirect.com/science/article/pii/S2212827114011366>, doi:<https://doi.org/10.1016/j.procir.2014.10.079>. 5th CATS 2014 - CIRP Conference on Assembly Technologies and Systems, Patras, Greece.
- Nieuwenhuisen, M., Droschel, D., Holz, D., Stuckler, J., Berner, A., Li, J., Klein, R., Behnke, S., 2013. Mobile bin picking with an anthropomorphic service robot, in: 2013 IEEE International Conference on Robotics and Automation, IEEE, Karlsruhe, Germany. pp. 2327–2334. doi:10.1109/icra.2013.6630892.
- Pedrocchi, N., Vicentini, F., Matteo, M., Tosatti, L.M., 2013. Safe human-robot cooperation in an industrial environment. International Journal of Advanced Robotic Systems 10, 27. URL: <https://doi.org/10.5772/53939>, doi:10.5772/53939, arXiv:<https://doi.org/10.5772/53939>.
- Pedrosa, E., Lim, G.H., Amaral, F., Pereira, A., Cunha, B., Azevedo, J.L., Dias, P., Dias, R., Reis, L.P., Shafii, N., Tudico, A., Mazzotti, C., Carricato, M., Badini, S., Rea, D., Lau, N., 2020. TIMAIRIS: Autonomous Blank Feeding for Packaging Machines. Springer International Publishing, Cham. pp. 153–186. URL: https://doi.org/10.1007/978-3-030-34507-5_7, doi:10.1007/978-3-030-34507-5_7.
- SAENZ, J., PENZLIN, F., VOGEL, C., FRITZSCHE, M., 2016. VALERI - A Collaborative Mobile Manipulator for Aerospace Production. WORLD SCIENTIFIC. pp. 186–195. URL: https://www.worldscientific.com/doi/abs/10.1142/9789813149137_0024, doi:10.1142/9789813149137_0024, arXiv:https://www.worldscientific.com/doi/pdf/10.1142/9789813149137_0024.
- Tsai, R.Y., Lenz, R.K., 1989. A new technique for fully autonomous and efficient 3d robotics hand/eye calibration. IEEE Transactions on Robotics and Automation 5, 345–358. doi:10.1109/70.34770.

- Unhelkar, V.V., Dörr, S., Bubeck, A., Lasota, P.A., Perez, J., Siu, H.C., Boerkoel, J.C., Tyroller, Q., Bix, J., Bartscher, S., Shah, J.A., 2018. Mobile robots for moving-floor assembly lines: Design, evaluation, and deployment. *IEEE Robotics Automation Magazine* 25, 72–81. doi:10.1109/MRA.2018.2815639.
- Weckx, S., Vandewal, B., Rademakers, E., Janssen, K., Geebelen, K., Wan, J., Geest, R.D., Perik, H., Gillis, J., Swevers, J., van Nunen, E., 2020. Open experimental AGV platform for dynamic obstacle avoidance in narrow corridors, in: 2020 IEEE Intelligent Vehicles Symposium (IV), IEEE. pp. 844–851. doi:10.1109/iv47402.2020.9304749.
- Yang, M., Yang, E., Zante, R.C., Post, M., Liu, X., 2019. Collaborative mobile industrial manipulator: A review of system architecture and applications, in: 2019 25th International Conference on Automation and Computing (ICAC), IEEE, Lancaster, United Kingdom. pp. 1–6. doi:10.23919/iconac.2019.8895183.
- Zhang, W., van Luttervelt, C., 2011. Toward a resilient manufacturing system. *CIRP Annals* 60, 469–472. URL: <https://www.sciencedirect.com/science/article/pii/S0007850611000424>, doi:<https://doi.org/10.1016/j.cirp.2011.03.041>.
- Zhang, Z., 2000. A flexible new technique for camera calibration. *IEEE Transactions on Pattern Analysis and Machine Intelligence* 22, 1330–1334. doi:10.1109/34.888718.